Spectrochimica Acta Part A 74 (2009) 849–854

Contents lists available at ScienceDirect

Spectrochimica Acta Part A: Molecular and Biomolecular Spectroscopy

journal homepage: www.elsevier.com/locate/saa

Electrochemical, catalytic and antimicrobial activities of N-functionalized cyclam based unsymmetrical dicompartmental binuclear nickel(II) complexes

S. Sreedaran[a], K. Shanmuga Bharathi[a], A. Kalilur Rahiman[a], R. Suresh[a], R. Jegadeesh[b], N. Raaman[b], V. Narayanan[a,*]

[a] Department of Inorganic Chemistry, School of Chemical Sciences, University of Madras, Guindy Campus, Chennai 600 025, Tamil Nadu, India
[b] Centre for Advanced Studies in Botany, University of Madras, Guindy Campus, Chennai 600 025, Tamil Nadu, India

ARTICLE INFO

Article history:
Received 28 December 2008
Received in revised form 3 July 2009
Accepted 5 August 2009

Keywords:
Dicompartmental ligand
Cyclam
Nickel(II) complexes
Hydrolysis of nitrophenylphosphate
Cyclic voltammetry
Antifungal activity

ABSTRACT

Five binuclear nickel(II) complexes have been prepared by simple Schiff base condensation of the compound 1,8-[bis(3-formyl-2-hydroxy-5-bromo)benzyl]-l,4,8,11-tetraazacyclotetradecane (L) with appropriate aliphatic or aromatic diamine, nickel(II) perchlorate and triethylamine. All the complexes were characterized by elemental and spectral analysis. Positive ion FAB mass spectra show the presence of dinickel core in the complexes. The electronic spectra of the complexes show red shift in the d–d transition. Electrochemical studies of the complexes show two irreversible one electron reduction processes in the range of 0 to −1.4 V. The reduction potential of the complexes shifts towards anodically upon increasing chain length of the macrocyclic ring. All the nickel(II) complexes show two irreversible one electron oxidation waves in the range 0.4–1.6 V. The observed rate constant values for catalysis of the hydrolysis of 4-nitrophenyl phosphate are in the range of 1.36×10^{-2}–9.14×10^{-2} min^{-1}. The rate constant values for the complexes containing aliphatic diimines are found to be higher than the complexes containing aromatic diimines. Spectral, electrochemical and catalytic studies of the complexes were compared on the basis of increasing chain length of the imine compartment. All the complexes show higher antimicrobial activity than the ligand and metal salt.

1. Introduction

N-functionalized cyclam ligands exhibit very rich coordination chemistry with a variety of transition metal ions [1,2]. The properties of these ligands can, in principle, be modified by varying the donor groups, size of the macrocycle, nature of the metal ions, etc. By this way the ligand assemblies can be tuned to give control over various aspects of metal–metal interactions, redox properties and exogenous ligand binding. There is currently intense interest in dinickel phenolate-bridged complexes as models for the active sites in enzymes [3,4]. The design of dinucleating compartmental ligands, whose two metal-binding sites are unsymmetrical with respect to the cavity size, coordination number, geometric requirement, or the nature of the donor atom, can serve as a muse for the bioinorganic chemist to inspire the generation of a range of bio-resemblant coordination chemistry [5]. These unsymmetrical compartmental ligands provide adjacent, dissimilar binding sites which can each accommodate a metal and so produce binuclear complexes with coordination environments resembling the active site in urease [6–8]. Hence, synthesis of model compounds that mimic the physical and chemical properties of the active sites present in metalloenzymes is very essential and the studies on such compounds is becoming increasingly important in understanding biological functions of the bimetallic cores [9].

Several N-functionalized macrocyclic systems bearing tetra and hexa coordination sites have been discussed (Chart I) in the literature [10]. Our research focuses on the synthesis of unsymmetrical dicompartmental ligands (Chart I) bearing N-functionalized cyclam groups (Scheme 1). This ligand contains hexa (N_4O_2, amine compartment) and tetra (N_2O_2, imine compartment) coordination sites. In these systems, one metal is in 6-coordinate site and the other is in 4-coordinate site, if a ligand like ClO_4^- is coordinated, this site can be made 5-coordinate. The advantage of this ligand is that the macrocyclic ring size can be controlled in order to study the spectral, electrochemical, catalytic properties. Additionally the presence of high valued cyclam group allows us to use these ligands and their complexes as potential antimicrobial agents.

2. Experimental

2.1. Analytical and physical measurements

Elemental analysis of the complexes was obtained using Haereus CHN rapid analyzer. ^{1}H NMR spectra were recorded using

* Corresponding author. Tel.: +91 44 2230 0488; fax: +91 44 2230 0488.
E-mail address: vnnara@yahoo.co.in (V. Narayanan).

1386-1425/$ – see front matter © 2009 Elsevier B.V. All rights reserved.
doi:10.1016/j.saa.2009.08.008

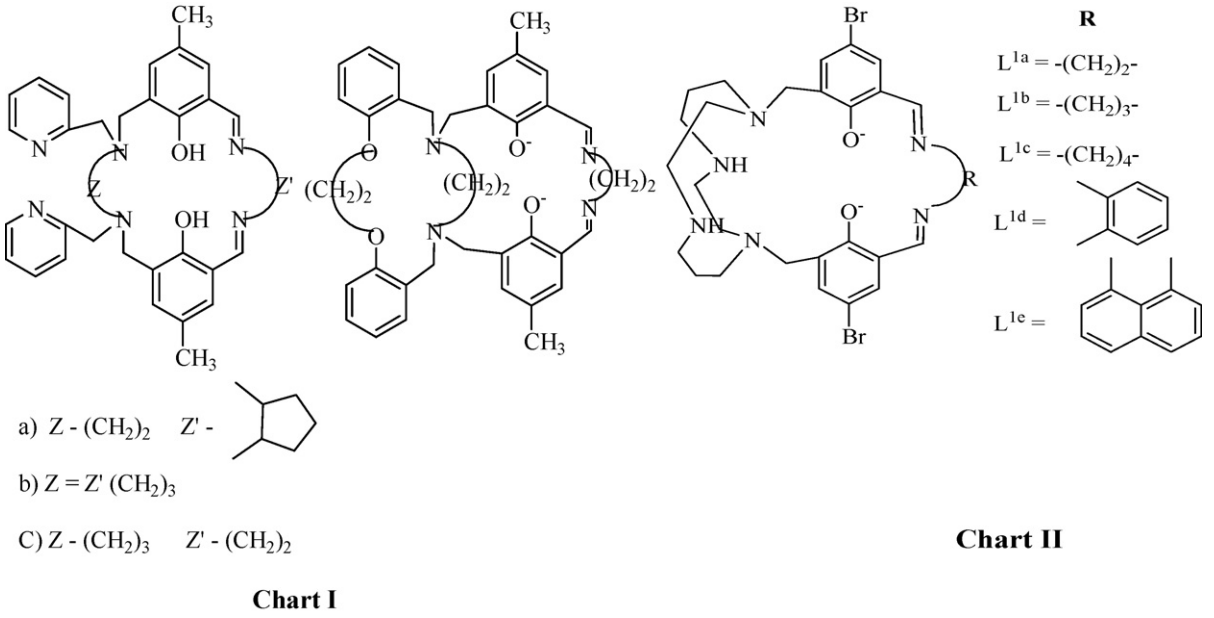

Chart I.

JEOL GSX 400 MHz NMR spectrometer. Electronic spectral studies were carried out on a Hitachi 320 spectrophotometer in the range 200–1100 nm. IR spectra were recorded on a Shimadzu FTIR 8300 series spectrophotometer on KBr disks in the range 4000–400 cm^{-1}. Molar conductivity was measured by using an Elico digital conductivity bridge model CM-88 using freshly prepared solution of the complex in dimethylformamide. The atomic absorption spectral data were recorded using Varian spectra AA-200 model atomic absorption spectrophotometer. Mass spectra were obtained on a JEOL SX-102 (FAB) mass spectrometer. Cyclic voltammograms were obtained on CHI-600A electrochemical analyzer. The measurements were carried out under oxygen free condition using a three-electrode cell in which a glassy carbon electrode was the working electrode, a saturated Ag/AgCl electrode was the reference electrode and platinum wire was used as the auxiliary electrode. A ferrocene/ferrocenium (1+) couple was used as an internal standard and $E_{1/2}$ of the ferrocene/ferrocenium (Fc/Fc^+) couple under the experimental condition is 470 mV. Tetra(n-butyl)ammonium perchlorate (TBAP) was used as the supporting electrolyte. Room temperature magnetic moment was measured on a PAR vibrating sample magnetometer Model-155. The hydrolysis of 4-nitrophenylphosphate by the nickel(II) complexes were

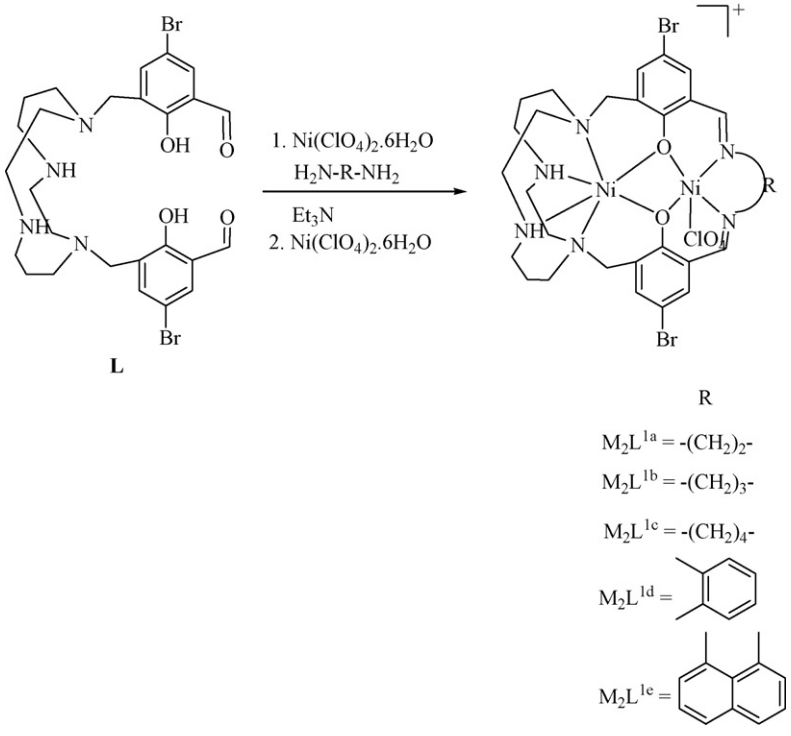

Scheme 1.

studied in a 10^{-3} M dimethylformamide by spectrophotometrically.

2.1.1. Chemicals and reagents

3-Chloromethyl-5-bromolsalicylaldehyde [11], 1,4,8,11-tetraazatricyclo[9.3.1.1^{4,8}]hexadecane [12] and 1,8-[bis(3-formyl-2-hydroxy-5-brmol)benzyl]-4,11-diazaniatricyclo[9.3.1.1^{4,8}]hexadecane dichloride [13] were prepared by following the literature method using 5-bromo salicylaldehyde instead of 5-methyl salicylaldehyde. 5-Bromo salicylaldehyde, analytical grade methanol, acetonitrile and dimethylformamide were purchased from Qualigens and used as such. TBAP used as supporting electrolyte in electrochemical measurement was purchased from Fluka and recrystallized from hot methanol. (*Caution!* TBAP is potentially explosive; hence care should be taken in handling the compound). All other chemicals and solvents were of analytical grade and were used as received without any further purification.

2.2. Synthesis of ligand (L)

2.2.1. Synthesis of 1,8-[bis(3-formyl-2-hydroxy-5-bromo)benzyl]-1,4,8,11-tetraazacyclotetradecane (L)

The compound 1,8-[bis(3-formyl-2-hydroxy-5-bromo)benzyl]-4,11-diazaniatricyclo[9.3.1.1^{4,8}]hexadecane dichloride (1 g, 0.0014 mol) was dissolved in 200 ml of an aqueous NaOH solution (0.3 M) with stirring. After stirring for 4 h, the solution was extracted with $CHCl_3$ (5×30 mL). The combined $CHCl_3$ extracts were dried with anhydrous $MgSO_4$, and concentrated under vacuum to give the expected compound 1,8-[bis(3-formyl-2-hydroxy-5-bromo)benzyl]-1,4,8,11-tetraazacyclotetradecane. Yield: 75%; m.p.: 300 °C (dec). Analytical data for $C_{26}H_{34}N_4O_4Br_2$: Calculated: C, 49.86; H, 5.47; N, 8.95; Found: C, 49.78; H, 5.42; N, 8.87. Selected IR (KBr): 3407 cm^{-1} ν(OH), 3289 cm^{-1} ν(NH), 1680 cm^{-1} ν(C=O); ^{1}H NMR δ (ppm in $CDCl_3$): 1.49 (q, 4H, β-CH_2), 2.56 (br, s, 2H, NH), 2.38 (m, 8H, α-CH_2), 3.39 (s, 8H, H_2C–N–CH_2) 4.1 (s, 4H, N–CH_2–Ar), 7.76 (d, 4H, Ar–H), 10.20 (s, 2H, Ar–CHO), 12.64 (br, s, Ar–OH). ^{13}C NMR δ (ppm in DMSO-D_6): 29.8, 49.7, 53.7, 55.0, 55.6, 61.6 122.6, 124.8, 126.0, 131.0, 136.1, 159.0, 196. λ_{max}, nm (ε, M^{-1} cm^{-1}) in DMF: 289 (22,760).

2.3. Synthesis of the macrobicyclic binuclear nickel(II) complexes

2.3.1. $[Ni_2L^{1a}(ClO_4)](ClO_4)$

A methanolic solution of nickel(II) perchlorate hexahydrate (0.74 g, 0.002 mol) was added to a hot solution of ligand component (L) (1.00 g, 0.002 mol) in methanol, followed by the addition of 1,2-diaminoethane (0.12 g, 0.002 mol) and triethylamine (0.41 g, 0.004 mol) in methanol. After an hour, another 1 equiv. of nickel(II) perchlorate (0.74 g, 0.002 mol) was added and the solution was refluxed in a water bath for 24 h. The resulting solution was filtered whilst hot and allowed to stand at room temperature. After slow evaporation of the solvent at 25 °C, dark green compound was collected by filtration, which was recrystallised in acetonitrile, and dried in vacuum.

2.3.2. $[Ni_2L^{1a}(ClO_4)](ClO_4)$

Dark green compound. Yield: 1.00 g (65%). Analytical data for $C_{28}H_{36}N_6O_{10}Cl_2Br_2Ni_2$: Calculated (%): C, 34.86; H, 3.76; N, 8.71; Ni, 12.17; Found (%): C, 34.83; H, 3.74; N, 8.69; Ni, 12.15; FAB mass (m/z) (%): $[Ni_2L^{1a}(ClO_4)\text{-}ClO_4]^+$ 865; conductance (Λ_m, S cm^2 mol^{-1}) in DMF: 75. Selected IR data (KBr) (ν/cm^{-1}): 3355 ν(NH), 1630 [s, ν(C=N)], 1107, 1105 (w) [$\nu(ClO_4^-)$ coordinated], 1100 (w) [$\nu(ClO_4^-)$ uncoordinated], 630 (s).

2.3.3. $[Ni_2L^{1b}(ClO_4)](ClO_4)$

Dark green compound. Yield: 0.97 g (62%). Analytical data for $C_{29}H_{38}N_6O_{10}Cl_2Br_2Ni_2$: Calculated (%): C, 35.59; H, 3.91; N, 8.57; Ni, 11.99; Found (%): C, 35.57; H, 3.89; N, 8.60; Ni, 11.96; conductance (Λ_m, S cm^2 mol^{-1}) in DMF: 78; selected IR data (KBr) (ν/cm^{-1}): 3349 ν(NH), 1634 [s, ν(C=N), 1092, 1089 (w) [$\nu(ClO_4^-)$ coordinated], 1105 (w) [$\nu(ClO_4^-)$ uncoordinated], 629 (s).

2.3.4. $[Ni_2L^{1c}(ClO_4)](ClO_4)$

Dark green compound. Yield: 0.98 g (62%). Analytical data for $C_{30}H_{40}N_6O_{10}Cl_2Br_2Ni_2$: Calculated (%): C, 36.30; H, 4.06; N, 8.47; Ni, 11.82; Found (%): C, 36.28; H, 4.09; N, 8.44; Ni, 11.80; FAB mass (m/z) (%): $[Ni_2L^{1c}\text{–}2ClO_4]^+$ 794; Conductance (Λ_m, S cm^2 mol^{-1}) in DMF: 81; selected IR data (KBr) (ν/cm^{-1}): 3357 ν(NH), 1637 [s, ν(C=N)], 1098, 1091 (w) [$\nu(ClO_4^-)$ coordinated], 1101 (w) [$\nu(ClO_4^-)$ uncoordinated], 624 (s).

2.3.5. $[Ni_2L^{1d}(ClO_4)](ClO_4)$

Dark green compound. Yield: 1.03 g (63%). Analytical data for $C_{32}H_{36}N_6O_{10}Cl_2Br_2Ni_2$: Calculated (%): C, 37.93; H, 3.58; N, 8.30; Ni, 11.59; Found (%): C, 37.90; H, 3.56; N, 8.33; Ni, 11.57; FAB mass (m/z) (%): $[Ni_2L^{1d}ClO_4\text{–}ClO_4]^+$ 913; Conductance (Λ_m, S cm^2 mol^{-1}) in DMF: 95; Selected IR data (KBr) (ν/cm^{-1}): 3335 ν(NH), 1643 [s, ν(C=N)], 1098, 1087 (w) [$\nu(ClO_4^-)$ coordinated], 1110 (w) [$\nu(ClO_4^-)$ uncoordinated], 626 (s).

2.3.6. $[Ni_2L^{1e}(ClO_4)](ClO_4)$

Dark green compound. Yield: 0.93 g (55%). Analytical data for $C_{36}H_{38}N_6O_{10}Cl_2Br_2Ni_2$: Calculated (%): C, 40.68; H, 3.60; N, 7.91; Ni, 11.04; Found (%): C, 40.66; H, 3.57; N, 7.94; Ni, 11.00; Conductance (Λ_m, S cm^2 mol^{-1}) in DMF: 95; Selected IR data (KBr) (ν/cm^{-1}): 3300 ν(NH), 1650 [s, ν(C=N), 1091, 1087 (w) [$\nu(ClO_4^-)$ coordinated], 1103 (w) [$\nu(ClO_4^-)$ uncoordinated], 626 (s).

3. Results and discussion

Five macrocyclic binuclear nickel(II) complexes were synthesized by Schiff's base condensation of the ligand with diamines in presence of metal ion (Scheme 1). In all the prepared nickel(II) complexes, one of the nickel(II) ion in the amine compartment is six coordinated, and the other in the imine compartment is five coordinated. Conductivity measurements of (Λ_m, 75–95 S cm^2 mol^{-1}) all the complexes show that they are 1:1 conductors in DMF solution [14]. The effective magnetic moment values for the nickel(II) complexes at room temperature are in the range of 2.58–2.74μ_B which is normally observed for octahedral coordinated nickel(II) ions due to the presence of strong nickel–nickel interaction. All attempts to grow single crystals of the complexes (e.g. by the diffusion of

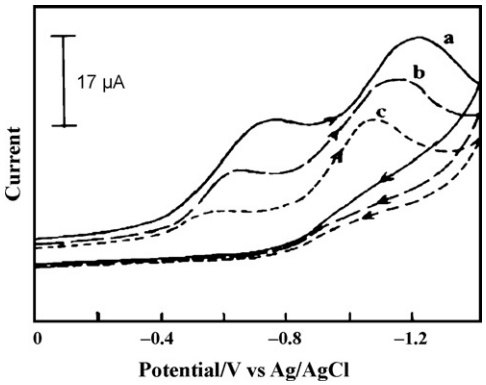

Fig. 1. Cyclic voltammogram of the complexes: (a) $[Ni_2L^{1a}(ClO_4)](ClO_4)$, (b) $[Ni_2L^{1b}(ClO_4)](ClO_4)$ and (c) $[Ni_2L^{1c}(ClO_4)](ClO_4)$ (reduction process).

Table 1
Electronic spectral data of binuclear nickel(II) complexes.

No.	Complexes	λ_{max}, nm (ε, M^{-1} cm^{-1})	
		d–d	Charge transfer
1	$[Ni_2L^{1a}(ClO_4)](ClO_4)$	985 (42), 726 (101), 612 (278)	382 (10 800), 300(17 600)
2	$[Ni_2L^{1b}(ClO_4)](ClO_4)$	1022 (50), 708 (87), 658 (164)	396 (10 700), 315 (18 400)
3	$[Ni_2L^{1c}(ClO_4)](ClO_4)$	1048 (34), 850 (75), 704 (205)	421 (11 900), 342 (15 200)
4	$[Ni_2L^{1d}(ClO_4)](ClO_4)$	956 (63), 730 (68), 600 (193)	371 (14 300), 304 (18 200)
5	$[Ni_2L^{1e}ClO_4)](ClO_4)$	995 (55), 756 (85), 690 (178)	373 (13 600), 305 (21 00)

Table 2
Electrochemical* and hydrolysis of 4-nitrophenylphosphate** data for the complexes.

No.	Complexes	Reduction (at cathodic)		Oxidation (at anodic)		Rate constant (k)
		E^1_{pc} (V)	E^2_{pc} (V)	E^1_{pc} (V)	E^2_{pc} (V)	($\times 10^{-2}$ min^{-1})
1	$[Ni_2L^{1a}(ClO_4)](ClO_4)$	−0.79	−1.23	0.86	1.22	5.85
2	$[Ni_2L^{1b}(ClO_4)](ClO_4)$	−0.64	−1.17	0.95	1.26	7.48
3	$[Ni_2L^{1c}(ClO_4)](ClO_4)$	−0.60	−1.10	0.98	1.36	9.14
4	$[Ni_2L^{1d}(ClO_4)](ClO_4)$	−0.77	−1.24	0.77	1.23	1.36
5	$[Ni_2L^{1e}ClO_4)](ClO_4)$	−0.60	−1.18	0.84	1.32	3.09

*Measured by CV at 50 mV/s E vs Ag/AgCl conditions: GC working and Ag/AgCl reference electrodes; supporting electrolyte TBAP; concentration of complex 1×10^{-3} M, concentration of TBAP 1×10^{-1} M. **Measured spectrophotometrically in DMF. Concentration of the complexes: 1×10^{-3} M. Concentration of 4-nitrophenylphosphate: 1×10^{-1} M. The rate constant values are the average of three experiments.

diethyl ether vapor into DMF solutions or recrystallization of the complexes from acetonitrile) have failed and only green powder or micro-crystals were obtained. Spectral, electrochemical, catalytic and antimicrobial studies of the complexes were carried out.

3.1. Spectral studies

The FT IR spectra of the binuclear nickel(II) complexes show bands in the region 3300–3357 cm^{-1}, indicating the presence of NH groups in the complexes. The IR spectra of ligand L shows a band at 1680 cm^{-1} due to the presence of C=O (–CHO) group. All the complexes show a sharp band in the region of 1630–1650 cm^{-1} due to the presence of C=N in the complexes. The complete disappearance of C=O peak (–CHO) and the appearance of a new C=N peak shows the effective Schiff base condensation between the aldehyde and the amines [15–17]. All the binuclear nickel(II) complexes showed two sharp peaks at near 1100 cm^{-1} and in the region of 624–630 cm^{-1}, which are assigned to perchlorate ions [18]. The peak around 1100 cm^{-1} is split, which clearly explains the presence of a coordinated perchlorate ion [19], while the other peak which does not show any splitting, indicate the presence of an uncoordinated perchlorate ion. The IR spectral data of the complexes show the presence of two different types of perchlorate ions. Further, the appearance of new bands in the 1537–1555 cm^{-1} region in all the complexes suggests phenoxide bridging with the metal ions [20].

Electronic spectra of five dinickel complexes were obtained in DMF medium (Table 1). The electronic spectra of all the complexes exhibit three main features. (i) One or two peaks in the range of 300–342 nm is assigned to the intra-ligand charge transfer transition (π–π^*). (ii) An intense peak in the range of 371–421 nm is due to ligand-to-metal charge transfer transition, and (iii) the d–d transition for the nickel(II) complexes show three main bands in the range of 612–1048 nm, which is characteristic of Ni^{2+} in the 5/6 coordination environment [21]. Although the appearance of the spectra bear similarities with those for octahedrally coordinated Ni(II) ions, the assignment of the three most intense bands $^3A_{2g} \rightarrow {}^3T_{2g}(P)$, $^3A_{2g} \rightarrow {}^3T_{1g}(F)$, $^3A_{2g} \rightarrow {}^3T_{1g}(P)$ to the spin allowed transitions of an octahedrally coordinated d^8 [21] ion would be a misinterpretation. Further, the higher molar extinction coefficients of the absorption band maxima in fact indicate a square pyramidal or trigonal bipyramidal coordination environment of at least one of the nickel(II) ions [21]. The electronic spectral studies inferred that an increase in λ_{max} (red shift) of the d–d transition of nickel(II) ion in the ligand L^{1a} to L^{1c} and L^{1d} to L^{1e}. This is due to the flexibility of the macrocyclic ring that is imparted by the distortion of the geometry of the complexes due to the increase in macrocyclic ring size, which causes more distortion of the geometry [22,23].

3.2. Electrochemical properties of the complexes

3.2.1. Reduction process at negative potential

The electrochemical data of the complexes are summarized in Table 2. The electrochemical behavior was studied by cyclic voltammetry in DMF containing 10^{-1} M tetra(n-butyl)ammonium perchlorate over the range of 0 to −1.30 V. Cyclic voltammograms for the complexes are shown in Fig. 1. The macrocyclic doubly phenoxo-bridged dinickel complexes typically undergo two well-separated one electron reductions [24,25]. It is observed that all the binuclear complexes show two irreversible reduction waves in the cathodic potential region. The first reduction potential ranges from −0.60 to −0.79 V and the second reduction potential lies in the range of −1.10 to −1.24 V. Controlled potential electrolysis

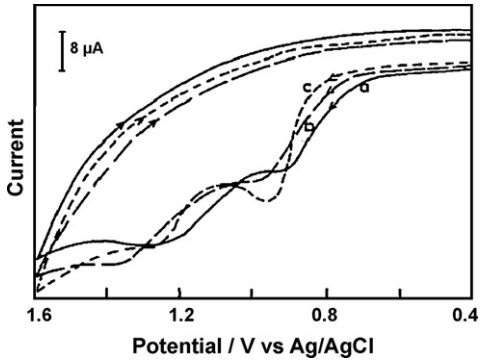

Fig. 2. Cyclic voltammogram of the complexes: (a) $[Ni_2L^{1a}(ClO_4)](ClO_4)$, (b) $[Ni_2L^{1b}(ClO_4)](ClO_4)$ and (c) $[Ni_2L^{1c}(ClO_4)](ClO_4)$ (oxidation process).

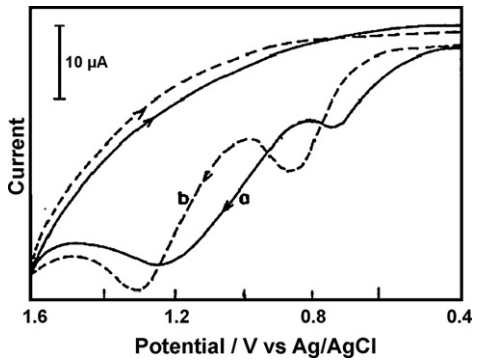

Fig. 3. Cyclic voltammogram of the complexes: (a) $[Ni_2L^{1d}ClO_4)](ClO_4)$ and (b) $[Ni_2L^{1e}(ClO_4)](ClO_4)$ (oxidation process).

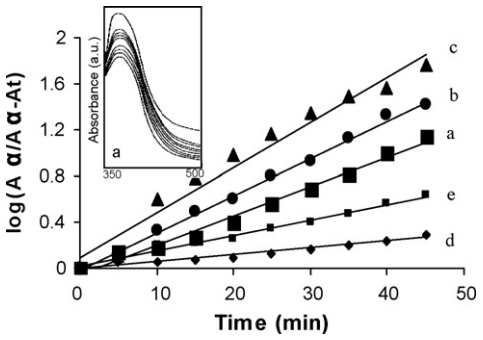

Fig. 4. Hydrolysis of 4-nitrophenylphosphate by binuclear nickel(II) complexes: (a) $[Ni_2L^{1a}(ClO_4)](ClO_4)$, (b) $[Ni_2L^{1b}(ClO_4)](ClO_4)$, (c) $[Ni_2L^{1c}(ClO_4)](ClO_4)$, (d) $[Ni_2L^{1d}(ClO_4)](ClO_4)$ and (e) $[Ni_2L^{1e}(ClO_4)](ClO_4)$. The inset is the time dependent growth of p-nitrophenolate chromophore in the presence of $[Ni_2L^{1a}(ClO_4)](ClO_4)$.

was also carried out and the experiment reports that each couple corresponds to one electron transfer process. The two reduction processes are assigned as follows:

$$Ni^{II}Ni^{II} \rightarrow Ni^{II}Ni^{I} \rightarrow Ni^{I}Ni^{I}$$

The first reduction potential of the Ni^{2+}/Ni^{+} couple for the complexes of L^{1a-c} in the range of −0.60 to −0.79 (Table 2) are attributed to the reduction of nickel(II) in the imine compartment (N_2O_2). The second reduction wave for the nickel(II) complexes of L^{1a-c} in the range −1.10 to −1.23 V, is attributed reduction of nickel(II) ion in the amine compartment (N_4O_2) [25]. From the result it is observed that, both first and second reduction potentials shift towards anodically, from −0.79 to −0.60 V and from −1.23 to −1.10 V, respectively, as the number of methylene groups is increased [26–28]. For example, the reduction potential for the nickel(II) complex of L^{1a} is (E^1_{pc} −0.79 V and E^2_{pc} −1.23 V), which are more negative in comparison to those of the complex of L^{1b} (E^1_{pc} −0.64 V and E^2_{pc} −1.17 V), which, in turn, are more negative in comparison to those of the complex of L^{1c} (E^1_{pc} −0.60 V and E^2_{pc} −1.10 V). This shows that as the chain length increases, the entire macrocyclic ring becomes more flexible, which causes easy reduction. Thus, the large size of the cavity easily holds the reduced cation and stabilizes the formation of Ni(I) in both compartments. The same trend is also observed for the complexes of the ligands L^{1d-e}. The reduction of complexes of L^{1d} and L^{1e} is rather difficult when compared to the reduction of the complexes of the ligands L^{1a-c} due to the planarity induced by the aromatic ring, which makes the system more rigid.

Further, the presence of electron-withdrawing substituent (Br) at the para position to the phenoxide oxygen in the phenyl ring plays an important role in the reduction process [29,30–33]. The nickel(II) complexes of the ligands L^{1a-e} reduced at lower negative potential than the complexes which contains electron donating ($-CH_3$) para substituent. This may be due to the poor electron donating nature of the bromide ion, which reduces the electron density on the metal ion [33b]. These results show that the magnitude of the bimetallic reduction process is subject to vary due to changes caused by the nature of the ligand, geometry and by the presence of the other metal [34].

3.2.2. Oxidation process at anodic potential

All the nickel complexes show two oxidation processes in the range 0.77–1.36 V. The cyclic voltammogram of the binuclear nickel(II) complexes are shown in Figs. 2 and 3 and the data are summarized in Table 2. The oxidation process is irreversible in nature. Controlled potential electrolysis experiment indicates that the two oxidation peaks are associated with stepwise oxidation process at nickel(II) center

$$Ni^{II}Ni^{II} \rightarrow Ni^{II}Ni^{III} \rightarrow Ni^{III}Ni^{III}$$

The first and second oxidation potential of the complexes of L^{1a-c} shifts towards more positive value [28] (from $E_{pc}{}^1$ 0.86 to 0.98 V and $E_{pc}{}^2$ 1.22 to 1.36 V) as the chain length increases in the imine compartment. This is because as the ring size increases due to flexibility, the planarity of the complex decreases and the electrochemical oxidation process occurs with difficult. For example the first and second oxidation potentials of the complex of L^{1c} is ($E_{pc}{}^1$ 0.98 and $E_{pc}{}^2$ 1.36 V) which are more positive when compared to the complex of L^{1b} ($E_{pc}{}^1$ 0.95 V and $E_{pc}{}^2$ 1.26 V) which is more positive than complexes of L^{1a} ($E_{pc}{}^1$ 0.86 V and $E_{pc}{}^2$ 1.22 V). Similar trend has been observed for complexes of L^{1d-e}. This is because for complexes with aromatic diimines, an increase in unsaturation will decrease the electron on the metal through delocalization, on to the ligand and this increases the difficulty to oxidize the metal ion.

3.3. Kinetic studies of hydrolysis of 4-nitrophenylphosphate

The catalytic activity of the nickel(II) complexes on the hydrolysis of 4-nitrophenylphosphate was determined spectrophotometrically by following our previous literature reports [29]. Plots of log ($A_\alpha/A_\alpha - A_t$) vs time for hydrolysis of 4-

Table 3
Antibacterial and antifungal screening data of complexes.

No	Complexes	Representation zone of inhibition (100 μg/ml)					
		Antibacterial					Antifungal
		S.a.	*B.c.*	*K.p.*	*P.a.*	*E.c.*	*C.a.*
1	$[Ni_2L^{1a}(ClO_4)](ClO_4)$	11	10	14	10	–	10
2	$[Ni_2L^{1b}(ClO_4)](ClO_4)$	13.5	11	10	14	–	11
3	$[Ni_2L^{1c}(ClO_4)](ClO_4)$	11	14.5	14	13.5	–	13
4	$[Ni_2L^{1d}(ClO_4)](ClO_4)$	12.5	13	12	19	–	17
5	$[Ni_2L^{1e}ClO_4)](ClO_4)$	14	14.5	15	17	–	18.5

S.a.: *Staphylococcus aureus*; *B.a.*: *Bacillus subtilis*; *K.p.*: *Klebsiella pneumonia*; *P.a.*: *Pseudomonas aeruginosa*; *E.c.*: *Escherichia coli*; *C.a.*: *Candida albicans*.

nitrophenylphosphate activity of the complexes are obtained and shown in Fig. 4. The observed initial rate constant values for all the nickel(II) complexes are given in Table 2. The observed rate constant values for catalysis of the hydrolysis of 4-nitrophenyl phosphate are in the range of 1.36×10^{-2}–9.14×10^{-2} min^{-1}.

The catalytic activities of the binuclear complexes are found to increase as the macrocyclic ring size increases due to the intrinsic flexibility, i.e. increase in the chelate ring size enhances the rate constant of hydrolysis fairly well by producing distortion in the geometry around the metal ion that enhances the accessibility of the metal ion for the bonding of phosphate and OH groups. The catalytic activity of the complexes containing aromatic diimines (L^{1d} and L^{1e}) is found to be less than that of the complexes containing aliphatic diimines. This may be due to the planarity, which is associated with aromatic ring, imparts less catalytic efficiency due to the rigidity of the systems as observed in the case of previous literature reports [35,36,10b]. It is seen that if the reduction potential is too negative, the complex has a decreased catalytic activity due to a more difficult reduction to metal(I), and a less negative reduction potential of the complex gives a higher catalytic activity since the donor atoms stabilize metal(I) at the expense of metal(II) [37].

The presence of electron-withdrawing substituent (Br) at the para position to the phenoxide oxygen in the phenyl ring is the reason for the observed higher hydrolysis activity than the complexes containing electron donating $-CH_3$ groups at the para position [30–33]. The literature reports [33b] also show that the complexes containing electron-withdrawing groups shows higher catalytic activity than complexes, which contain electron donating substituent.

3.4. Antimicrobial activities

Antifungal and antibacterial activities of the complexes were tested by following our earlier literature reports [29]. We have evaluated the antifungal activity of all the nickel(II) complexes against the human pathogenic fungus *Candida albicans*. The screening data were reported in Table 3. From the results, it is observed that all tested complexes show some antifungal activity comparable with the N-substituted tetraazamacrocycles [38]. The binuclear nickel(II) complexes of L^{1d} and L^{1e} show higher activity than the complexes of L^{1a} to L^{1c}, which contain aliphatic diimines.

All the nickel(II) complexes have also been screened for their in vitro antimicrobial activity against the human pathogenic bacteria gram (−) *Escherichia coli* (ATCC 11775), *Pseudomonas aeruginosa* (ATCC 10145), *Bacillus subtilis* (ATCC 6633), *Klebsiella pneumonia* (ATCC 13883) and gram (+) *Staphylococcus aureus* (ATCC 12600) by following our earlier method [29]. The screening results are given in Table 3. The complexes are all highly potent against *P. aeruginosa*, *B. subtilis*, *K. pneumonia* and *S. aureus*. All the complexes are inactive against *E. coli*. All the complexes show superior activity compared to the ligand L and nickel(II) perchlorate. All the complexes show good antibacterial activity compared to tetraazamacrocyclic nickel(II) complexes reported in the literature [38].

4. Conclusion

In conclusion, it has been observed that the presence of N-functionalized cyclam unit in the macrocycle does apparently improving the catalytic and antimicrobial activity. N-alkylation and the presence of para substituent of the phenoxide to the phenyl ring in the macrocycle also influence the electrochemical, magnetic and electronic spectra of the complexes.

Acknowledgements

Financial support from University Grants Commission (RGN-SRF), New Delhi, is gratefully acknowledged. We are thankful to CDRI-Lucknow for providing FAB Mass spectral analysis.

References

[1] F. Denat, S. Brandès, R. Guilard, Synlett 5 (2000) 561.
[2] P.V. Bernhardt, G.A. Lawrence, Coord. Chem. Rev. 104 (1990) 297.
[3] A. Volbeda, M.-H. Charon, C. Piras, E.C. Hatchikian, M. Frey, J.C. Fontecilla-Camps, Nature 373 (1995) 580.
[4] S. Brooker, P.D. Croucher, F.M. Roxburgh, J. Chem. Soc., Dalton Trans. (1996) 3031.
[5] E. Jabri, M.B. Carr, R.P. Hausinger, P.A. Karplus, Science 268 (1995) 998.
[6] T. Koga, H. Furutachi, T. Nakamura, N. Fukita, M. Ohba, K. Takahashi, H. Okawa, Inorg. Chem. 37 (1998) 989.
[7] S. Uozumi, H. Furutachi, M. Ohba, H. Okawa, D.E. Fenton, K. Shindo, S. Murata, D.J. Kitko, Inorg. Chem. 37 (1998) 6281.
[8] D.E. Fenton, Inorg. Chem. Commun. 5 (2002) 537.
[9] D.E. Fenton, H. Okawa, Perspectives on Bioinorganic Chemistry, JAI Press, London, 1993, p. 8.
[10] (a) E.V. Rybak-Akimova, N.W. Alcock, D.H. Bush, Inorg. Chem. 37 (1998) 1563; (b) M. Thirumavalavan, P. Akilan, M. Kandaswamy, K. Chinnakali, G. Senthil Kumar, H.K. Fun, Inorg. Chem. 42 (2003) 3308; (c) T.H. Ahn, J. Kim, L.F. Lindoy, J. Wang, Aust. J. Chem. 52 (1999) 1139.
[11] J.D. Gane, D.E. Fenton, J.M. Latour, A.J. Smith, J. Chem. Soc., Dalton Trans. (1991) 2279.
[12] G. Royal, V.D. Gindrey, S. Dahaowi, A. Tabard, R. Guilard, P. Pullumbi, C. Lecomte, Eur. J. Org. Chem. (1998) 1971.
[13] D. Gayathri, D. Velmurugan, K. Ravikumar, S. Sreedaran, V. Narayanan, Acta. Cyst. E62 (2006) o3714.
[14] J. Geary, Coord. Chem. Rev. 7 (1971) 81.
[15] G. Das, R. shukala, S. Mandal, R. Singh, P.K. Bharadwaj, J.V. Singh, K.H. Whitemine, Inorg. Chem. 36 (1997) 323.
[16] R.M. Silverstein, G.C. Bassler, Spectrometric Identification of Organic Compounds, John Wiley & Sons, New York, 1991.
[17] C. Fraser, R. Ostrander, A.L. Rheingold, C. White, B. Bosnich, Inorg. Chem. 33 (1994) 324.
[18] M. Lachkar, R. Guilard, A. Attamani, A.De. Clan, J. Fisher, R. Weiss, Inorg. Chem. 37 (1997) 1575.
[19] S.S. Tandon, L.K. Thompson, J.N. Bridson, V. Mekee, A.J. Downard, Inorg. Chem. 31 (1992) 4635.
[20] B. Srinivas, N. Arulsamy, P.S. Zacharias, Polyhedron 10 (1991) 731.
[21] (a) M.F. Cabral, B. Murphy, J. Nelson, Inorg. Chim. Acta 90 (1984) 169; (b) D. Volkmer, B. Hommerich, K. Griesar, W. Haase, B. Krebs, Inorg. Chem. 35 (1996) 3792.
[22] H. Okawa, S. Kida, Bull. Chem. Soc. Jpn. 45 (1972) 1759.
[23] H. Wada, T. Aono, K. Moodo, m. Ohba, N. Makstumoto, H. Okawa, Inorg. Chem. Acta 246 (1996) 13.
[24] A. Benzekeri, P. Dubourdeax, J.M. Latour, P. Rey, J. Laugier, J. Chem. Soc., Dalton Trans. (1991) 3359.
[25] (a) R.R. Gagne, L.M. Henling, T.J. Kistenmacher, Inorg. Chem. 19 (1980) 1226; (b) C. Fraser, B. Bosnich, Inorganics 41 (2002) 1788.
[26] F.V. Lovecchino, E.S. gore, D.H. Bush, J. Am. Chem. Soc. 96 (1974) 3104.
[27] G.K. Bareford, G.M. Freeman, D.G. Erver, Inorg. Chem. 86 (1986) 552.
[28] (a) G.A. Bowmaker, J.P. Williams, J. Chem. Soc., Dalton. Trans. (1993) 3593; (b) E. Gao, W. Bu, G. Yang, D. Liao, Z. Jiang, S. Yan, G. Wang, J. Chem. Soc., Dalton Trans. (2000) 1431.
[29] (a) S. Sreedaran, K.S. Bharathi, A.K. Rahiman, L. Jagadish, V. Kaviyarasan, V. Narayanan, Polyhedron 27 (2008) 2931; (b) S. Sreedaran, K.S. Bharathi, A.K. Rahiman, K. Rajesh, G. Nirmala, L. Jagadish, V. Kaviyarasan, V. Narayanan, Polyhedron 27 (2008) 1867.
[30] (a) J. Nishio, H. Okawa, S. Ohtsuka, M. Tomono, Inorg Chim. Acta 218 (1994) 27; (b) G.A. Melson (Ed.), Coordination Chemistry of Macrocyclic Compounds, Plenum Press, New York, 1979.
[31] (a) V. Alexander, Chem. Rev. 95 (1995) 273; (b) M. Yonemura, Y. Matsumura, H. Furutachi, M. Ohba, H. Okawa, D.E. Fenton, Inorg. Chem. 36 (1997) 2711.
[32] T.C. Higgs, C.J. Carrano, Inorg. Chem. 36 (1997) 298.
[33] (a) R. Mahalakshmy, R. Venkatesan, P.S. Sambasiva Rao, R. Kannappan, T.M. Rajendiran, Trans. Met. Chem. 29 (2004) 623; (b) M.J. Mac Lachlan, M.K. Park, L.K. Thompson, Inorg. Chem. 35 (1996) 5492.
[34] C. Belle, C. Beguin, I. luneau, S. Hamman, C. Philouze, J.L. Pierre, F. Thomas, S. Torelli, Inorg. Chem. 41 (2002) 479.
[35] J. Reim, B. Kreks, J. Chem. Soc., Dalton. Trans. (1997) 3793.
[36] P. Akilan, M. Thirumavalan, M. Kandaswamy, Polyhedron 22 (2003) 3483.
[37] P. Amudha, M. Kandaswamy, L. Govindasamy, D. Velmurugan, Inorg. Chem. 37 (1998) 4486.
[38] (a) M.A. Ali, A.H. Mirza, A. Monsur, S. Hossain, M. Nazimuddin, Polyhedron 20 (2001) 1045; (b) T.G. Roy, S.K.S. Hazari, B.K. Dey, H.A. Miah, C. Bader, D. Rehder, Eur. J. Inorg. Chem. (2004) 4115.